


**Please cite the Published Version**

Vadivel, Srinivasan, Ramasamy, Sridhar, Mikkili, Suresh, Ahsan, Mominul, Haider, Julfikar , Islam, Md Minarul and Ustun, Taha Selim (2023) Hybrid Social Grouping Algorithm-Perturb and Observe Power Tracking Scheme for Partially Shaded Photovoltaic Array. International Journal of Energy Research, 2023. p. 9905979. ISSN 0363-907X

**DOI:** <https://doi.org/10.1155/2023/9905979>

**Publisher:** Hindawi

**Version:** Published Version

**Downloaded from:** <https://e-space.mmu.ac.uk/632596/>

**Usage rights:**  [Creative Commons: Attribution 4.0](https://creativecommons.org/licenses/by/4.0/)

**Additional Information:** This is an Open Access article published in International Journal of Energy Research, by Hindawi.






**Data Access Statement:** No underlying data was collected or produced in this study.

**Enquiries:**

If you have questions about this document, contact [openresearch@mmu.ac.uk](mailto:openresearch@mmu.ac.uk). Please include the URL of the record in e-space. If you believe that your, or a third party's rights have been compromised through this document please see our Take Down policy (available from <https://www.mmu.ac.uk/library/using-the-library/policies-and-guidelines>)

## Research Article

# Hybrid Social Grouping Algorithm-Perturb and Observe Power Tracking Scheme for Partially Shaded Photovoltaic Array

Srinivasan Vadivel <sup>1</sup>, Sridhar Ramasamy <sup>2</sup>, Suresh Mikkili <sup>3</sup>, Mominul Ahsan,<sup>4</sup>  
Julfikar Haider <sup>5</sup>, Md. Minarul Islam <sup>6</sup> and Taha Selim Ustun <sup>7</sup>

<sup>1</sup>Department of Electronics and Instrumentation Engineering, SRM Valliammai Engineering College, Kattankulathur, Tamil Nadu, India

<sup>2</sup>Department of Electrical and Electronics Engineering, SRM Institute of Science and Technology, Kattankulathur, 603203 Tamil Nadu, India

<sup>3</sup>Department of Electrical and Electronics Engineering, National Institute of Technology Goa, 403401, Goa, India

<sup>4</sup>Department of Computer Science, University of York, Deramore Lane, York YO10 5GH, UK

<sup>5</sup>Department of Engineering, Manchester Metropolitan University, John Dalton Building, Chester Street, Manchester M1 5GD, UK

<sup>6</sup>Department of Electrical and Electronic Engineering, University of Dhaka, Dhaka 1000, Bangladesh

<sup>7</sup>Fukushima Renewable Energy Institute, AIST (FREIA), 2-2-9 Machiikedai, Koriyama, Fukushima 963-0298, Japan

Correspondence should be addressed to Sridhar Ramasamy; sridharr@srmist.edu.in, Md. Minarul Islam; mmislam-eee@du.ac.bd, and Taha Selim Ustun; selim.ustun@aist.go.jp

Received 18 May 2023; Revised 1 August 2023; Accepted 3 August 2023; Published 22 September 2023

Academic Editor: Subhashree Choudhury

Copyright © 2023 Srinivasan Vadivel et al. This is an open access article distributed under the Creative Commons Attribution License, which permits unrestricted use, distribution, and reproduction in any medium, provided the original work is properly cited.

This research work emphasizes proposing a hybrid social grouping algorithm (SGA) and perturb and observe (P&O) scheme for tracking the global power peak in a partially shaded photovoltaic (PV) array. PV panels getting shaded, even partially, exhibits multiple power peaks, and hence conventional maximum power point tracking (MPPT) algorithms fail in tracking the maximum power peak as it gets deceived by local maxima. Most of the prevailing global search algorithms suffer in performance due to the stochastic search which consumes time even after nearing the global power peak. Therefore, a hybridization of the global search algorithm and the conventional algorithm will be a prudent solution. SGA, a global search algorithm based on individual and group cognizant behaviour, has been hybridized with a well-entrenched P&O algorithm that complements each other in achieving the global power peak swiftly. The hybridized algorithm achieves the global power peak in 0.4 seconds faster than the stand-alone SGA algorithm during complex shading conditions. The proposed scheme has been implemented for an 800 W PV array in a MATLAB simulation and validated experimentally in a hardware setup using a SAS1000L solar array simulator-programmable source, a DC-DC converter, and a dSPACE 1104 controller. The simulation and experimental results reveal that the proposed search scheme is very competent in converging towards the global maximum through SGA first and achieving the peak point through P&O. The proposed scheme has also been tested for a dynamic shading pattern, and it is evident that the proposed scheme outperforms its counterparts in terms of convergence time.

## 1. Introduction

Global warming and climate change across the world have pushed countries to have the motto of one earth, one family, one future. Recently, the power production through the photovoltaic (PV) power system has become more pragmatic and

prominent due to its declined cost and improved efficiency [1]. As an example, India as a developing country has an ambitious target of adding nearly 20 GW of PV system deployment in the next five years. The major area of concern with the PV system is the power production from PV is not steady due to the intermittent nature of the solar irradiance [2].

The output characteristic power curves of the PV panels are nonlinear in nature, and the peak power of the curve varies with the environmental conditions, e.g., temperature and irradiation. For this reason, the maximum power point tracking (MPPT) is a mandatory scheme employed in PV systems to ensure the maximum power production at any environmental condition [3]. MPPT, a controller which possesses an algorithm and a converter, accurately renders the control signal in the appropriate operating voltage of the PV at which the peak power exists [4]. In the research arena, numerous MPPT schemes are available [5]. The incremental conductance (INC) though competent in tracking DC peak power without oscillation is relatively used lesser than the perturb and observe (P&O) for its complex coding [6]. P&O remains be most coveted MPPT because the algorithm execution is more reliable and relatively easier [7].

Other interesting offline MPPT schemes such as open circuit voltage (OCV) and short circuit current (SCC) were also used for PV-fed standalone applications [8]. A fractional open circuit (FOCV) scheme uses an adaptive MPPT algorithm. But these schemes are not advisable for critical loads since the loads need to be isolated to calculate OCV and SCC [9]. Many research articles have been published with the modifications in the four algorithms mentioned above, i.e., INC, P&O, OCV, and SCC, which form the bar for all other MPPT schemes. Ali et al. have initiated a dynamic perturbation in step time during the search process to improve the tracking efficiency of a typical P&O power tracking scheme [10]. Another initiative by Shang et al. [11] to improve the performance of the INC MPPT was interesting. Here, the dynamic change of current and voltage along the slope of the power curve is better into account. Similarly, the approximate load intermittency issues in FOCV and SCC were addressed through control schemes which are adopted with the dynamic changes in the irradiance.

The PV system suffers major power loss when some of the PV panels get shaded even partially. Due to the shading effect, the cumulative P-V curves will exhibit multiple power peaks. These multiple power peaks are due to the bypass diodes in the PV string [12, 13]. These antiparallel bypass diodes across the shaded panels facilitate a closed-loop path for the healthier panels which are not prone to shading. Under these conditions, the conventional MPPT algorithm which performs a linear search over the P-V curve gets stuck to the first local power peak it encounters with. The global power peak is the one which results in higher power generation, whether it be fed to a load or injected into the grid. Due to the failure of the conventional search mechanism to find the global peak, on an average of 60-70% power loss occurs during partial shading [14]. To prevail over these local and global power peak issues, a host of intelligent power tracking schemes which inherently possess global search mechanisms have been proposed in the literature. Particle swarm optimization (PSO) MPPT is a well-established scheme [15–18] where the particles are randomly initiated in the search space, and these particle positions get velocity updated after each iteration. During each iteration, the updated position information is shared between the particles to select the global and particle best. The PSO technique suffers in terms of convergence as random search

makes the search process cumbersome. The artificial bee colony (ABC) MPPT algorithm works on the foraging of honeybee phenomena through which peak power is tracked [19]. The convergence time as well as the peak power tracking capability of the ABC MPPT algorithm is better compared to PSO and emperor penguin optimization (EPO) methods [20]. Similar work by Abou et al. [21] also ensured that ABC is a better candidate in terms of accuracy in finding the global peak. Many global search algorithms have been advocated in the literature; among them, the most prominent algorithms are the grey wolf optimization (GWO) scheme, grasshopper optimization, honey badger algorithm, and bat algorithm where each of them has its own advantages and disadvantages [22–24].

The individual nature-inspired optimization algorithms experience a major setback in terms of reliable results. These heuristic algorithms possess a chance of acquiring different peak power values for each run, and therefore, the prudent choice would be hybridizing the intelligent algorithms with the conventional linear search algorithms. The intelligent PSO and the most prevalent P&O is hybridized for a 5S configuration by Veerapen et al. [25], and it is inferred that this hybridization was so fruitful as to yield an efficiency of 96.7%. The main drawback here is the initialization of random duty cycles which results in complex search procedure. Further research on PSO and P&O was modified into an accelerated one [26] where in the efficiency is 99% percent but the PV configuration used to test is a typical one. From [27], it is inferred that as many as three algorithms like grey wolf optimization (GWO), moth-flame optimization algorithm (MFO), and salp salt algorithm (SSA) are combined with geographical search algorithm (GSA) and compared with PSO-GSA algorithm. The PSO GSA algorithm renders better efficiency than other combinations. But here the implementation complexity gets doubled as both these algorithms need rigorous coding deployment. The hybrid P&O ABC [28] scheme is tested for a lower-rated PV array of 74 W, and though the scheme was effective with respect to convergence and tracking efficiency, the combination did not work out for a 2S PV array configuration. Another interesting work involving the bat algorithm with Bat-P&O MPPT, Bat-Beta MPPT, and Bat-IC MPPT has been proposed in [29], which advocates a quick convergence time of 5 seconds. The trigonometric convergence hybridization with GWO ensures fast tracking with improved efficiency [30], yet the boost full bridge topology suggested in this work does not hold good for all applications. Recently, a hybrid MPPT based on simulated annealing (SA) and PO MPPT [31] has been proposed, but the competence of the suggested algorithm was compared with only conventional MPPT schemes. From a detailed literature survey, it can be concluded that the hybrid MPPT approaches such as a social group and perturb and observe MPPT are the promising ones in terms of a number of parameters and convergence time. SGO algorithm known for its fast convergence and less oscillation was deployed by Vadivel et al. [32] for MPPT in a partially shaded PV array. The results of the work proved that the SGO is a very competent candidate for dynamically varying irradiation patterns. Hence, hybridizing SGO with a

conventional MPPT like P&O will be a prudent solution that has not been attempted in the research arena.

This paper proposes a social grouping and P&O MPPT which track the global power peak during both the shaded and nonshaded conditions which possess good tracking efficiency and convergence time. The novel aspects of this work can be listed as follows:

- (1) Hybridizing a well-enhanced conventional P&O with an inventive social group MPPT algorithm facilitates the reliability of the search process
- (2) The exploration and exploitation stages in the social grouping algorithm prove to be a better candidate for power tracking than its other global search counterparts

The remainder of the paper is organized as follows. The conceptualization of PV modeling and the characteristic features are shown in Section 2. Section 3 details the formulation of the optimization problem and the proposed hybrid SGO and P&O scheme. Other algorithms like SGO and P&O under static and dynamic partial shading conditions (PSCs) are presented in Section 4. Finally, the conclusions are given in Section 5.

## 2. PV Model and System Description

**2.1. PV Modeling.** The equivalent circuit model of a PV cell embodies a current source ( $I_{ph}$ ), a diode ( $D$ ), and a resistor ( $R_s$ ) in parallel with another resistor ( $R_p$ ). Each component has its own significance. The current source ( $I_{ph}$ ) represents the incident sunlight- (photo) generated current. Magnitude of the current relies on the intensity of the incident light and the conversion (light to current) efficiency of the solar cell. The diode ( $D$ ) in the PV cell model represents the p-n junction within the solar cell. When light strikes the p-n junction, a voltage across diode is generated due to electron-hole pair formation. This voltage will be maintaining the diode in reverse bias as and when the solar cell is generating electricity (forward bias). The series resistance ( $R_s$ ) is the representation of resistance present internally in the cell and refers also to the resistive losses. Due to this, a series voltage drop occurs, thereby reducing the effective voltage across the cell. The shunt resistance ( $R_p$ ) represents leakage paths or parasitic resistance that allow some current to bypass the diode and the series resistance. The comprehensive behaviour of the solar cell under different environmental conditions relies predominantly upon the impact of irradiation upon the current source, diode, series resistance, and shunt resistance. This PV model predicts the cell's electrical characteristics, such as current-voltage (I-V) and power-voltage (P-V) curves, which are vital for developing an efficient solar PV systems [33]. A typical nonideal PV cell is shown in Figure 1.

The photoelectric impact is directly proportional to the magnitude of the solar irradiation falls on the panel. The photoelectric impact is represented using a current source denoted by  $I_{ph}$ . which is used in the modelling process.

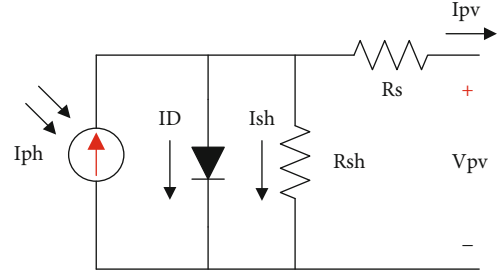


FIGURE 1: Single-diode PV equivalent circuit.

The leakage current flows through two distinct paths: first one is through a p-n junction that is denoted by  $I_d$ , and the second one is through a parallel resistor that is denoted by  $I_{sh}$ . The series resistor,  $R_s$ , takes into consideration the power that is being sacrificed from within the cell. Therefore, the output current  $I_{PV}$  from the PV cell can be expressed as in [34]

$$I_{PV} = I_{ph} - I_O \left\{ \exp \left[ \frac{(V_{PV} + I_{PV} * R_s)}{N_s * (\eta k_b T / q)} \right] - 1 \right\} - \frac{V_{PV} + I_{PV} * R_s}{R_{sh}}. \quad (1)$$

$I_O$  refers to the saturation current of the diode, whereas  $q$  is the electron charge ( $1.602 \times 10^{-19}$  C). The Boltzmann constant  $k$  is  $1.3806503 \times 10^{-23}$  J/K, and  $T$  is the cell temperature. The closeness of a practical diode and an ideal diode is given by the ideality factor  $\eta$ . The cells are arranged in series and parallel to constitute a PV panel of desired voltage and current.  $N_s$  and  $N_p$  refer to the number of cells connected in series and parallel, respectively.

To compute the total current produced by PV module under partial shading effect (1), it can be rewritten as in [35]

$$I_{PV} = N_p I_{ph} - I_O \left\{ \exp \left[ \frac{(V_{PV} + I_{PV} * R_s (N_s / N_p))}{N_s * (\eta k_b T / q)} \right] - 1 \right\} - \frac{V_{PV} + I_{PV} * R_s (N_s / N_p)}{(N_s / N_p) R_{sh}}. \quad (2)$$

**2.2. System Description.** The presence of bypass diodes across the PV panels in an array prevents the formation of hot spots but results in the introduction of multiple power peaks. Figure 2(a) shows a PV array topology in uniform and shaded irradiance conditions. The existence of several power peaks in the P-V curve for a 4-stage PV array topology is represented in Figure 2(b). The multiple power peaks symbolize the significance of the MPPT approaches. The global search algorithms, though prevail in acquiring the global power peak, possess the disadvantage in consistency and accuracy. When the shading pattern is very dynamic, the competency of the searching scheme is tested under different conditions and shows its real performance. Therefore, three distinct shading patterns are emulated in this paper. It is important to point out that identification of the global power peak by any MPPT approach is made significantly more difficult by

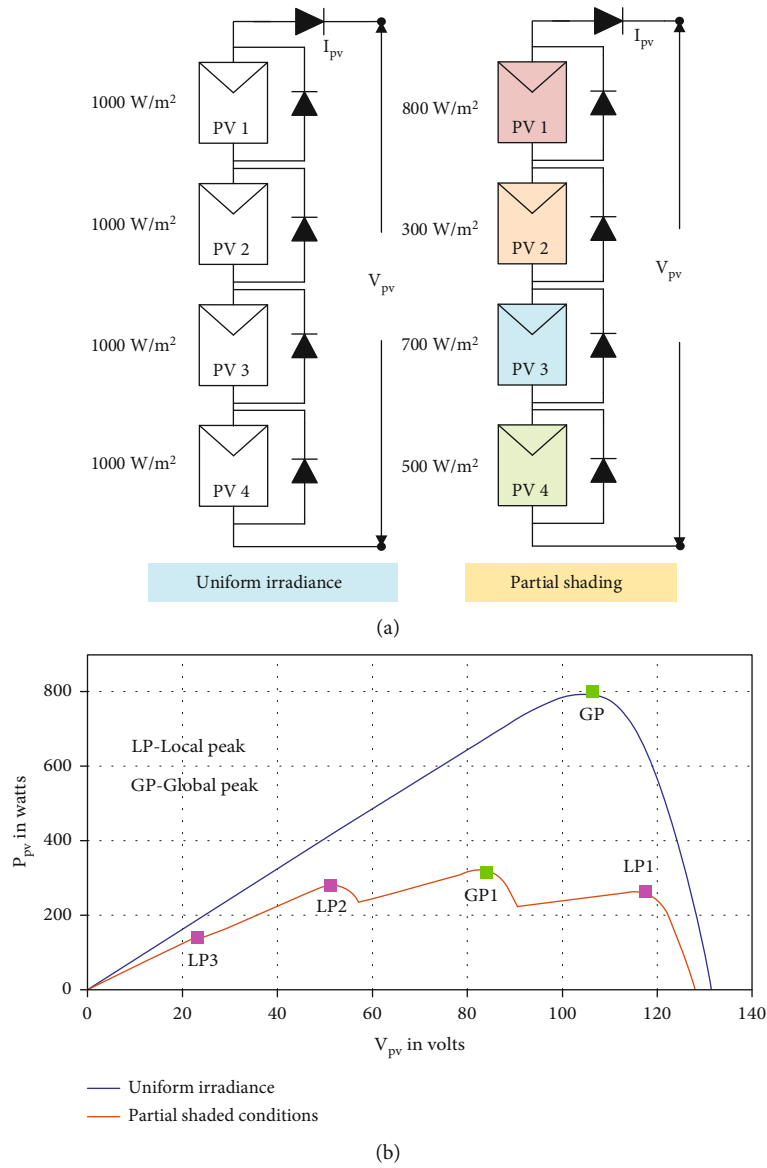


FIGURE 2: (a) 4-stage PV configuration. (b) P-V characteristics of uniform and PSC.

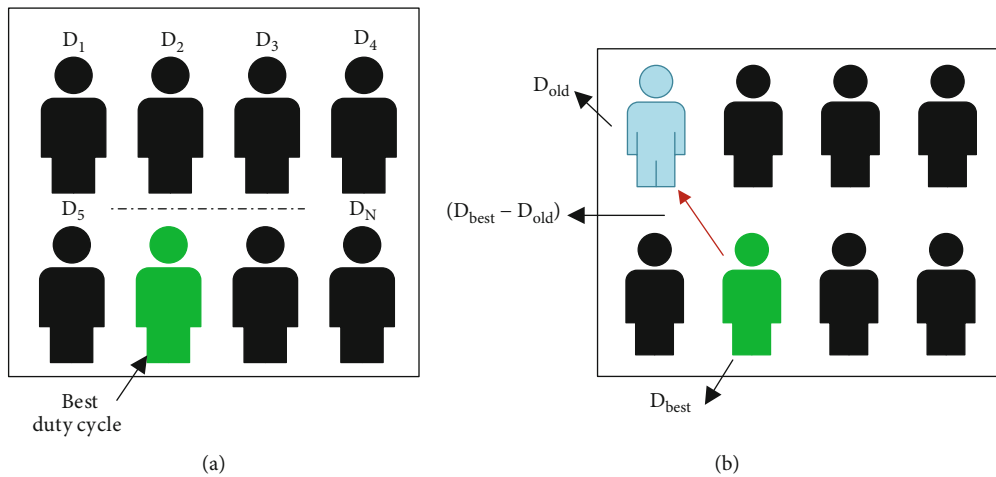


FIGURE 3: (a) Best candidate (best duty cycle) of the group. (b) Best fitness of the candidate in SGO algorithm.

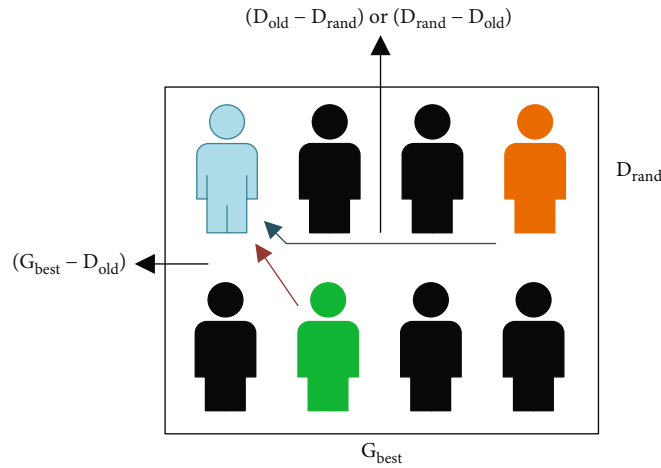


FIGURE 4:  $G_{best}$  candidate of the group in SGO algorithm.

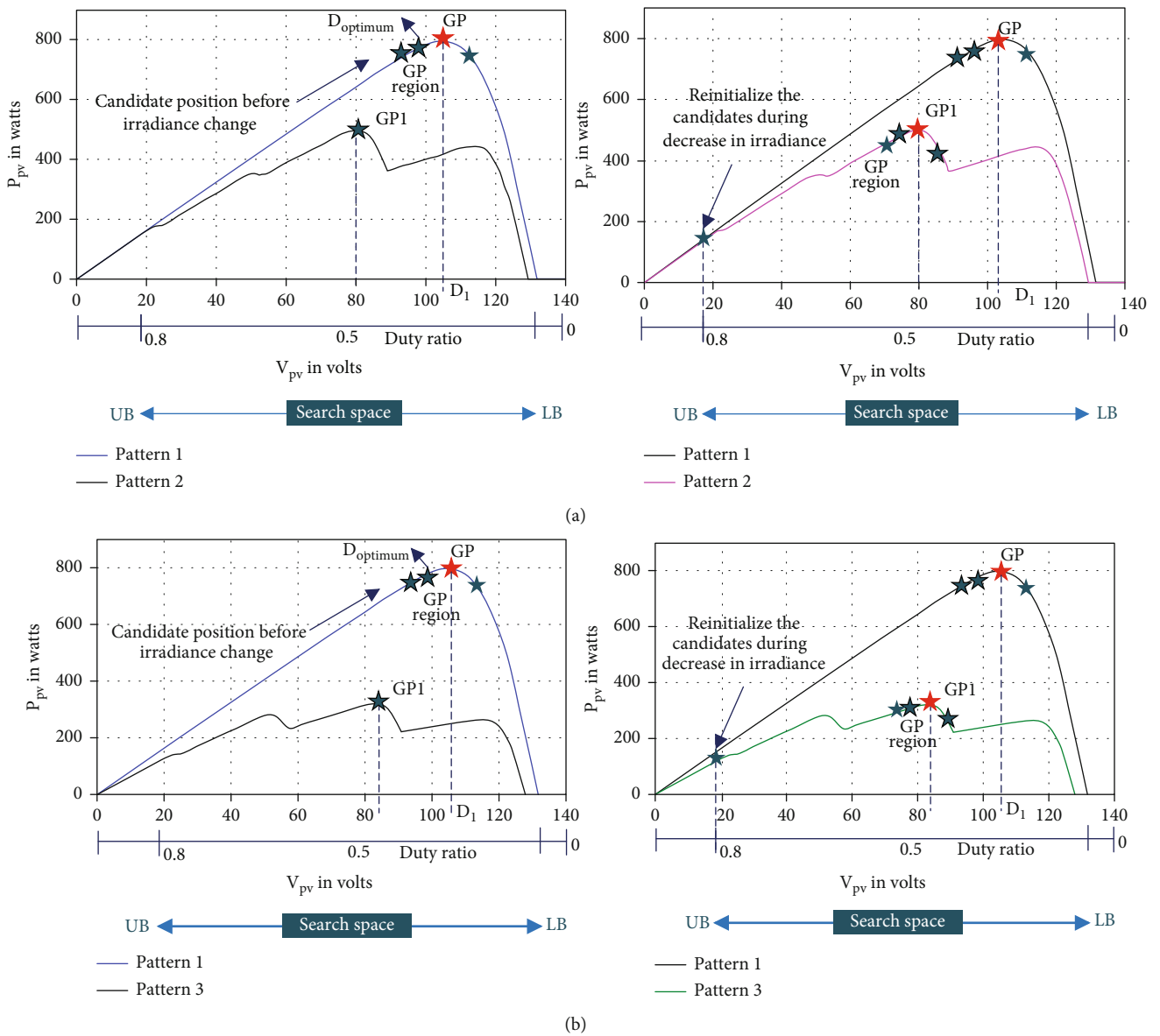


FIGURE 5: (a) Pattern 1 to pattern 2 irradiance change. (b) Pattern 1 to pattern 3 irradiance change.

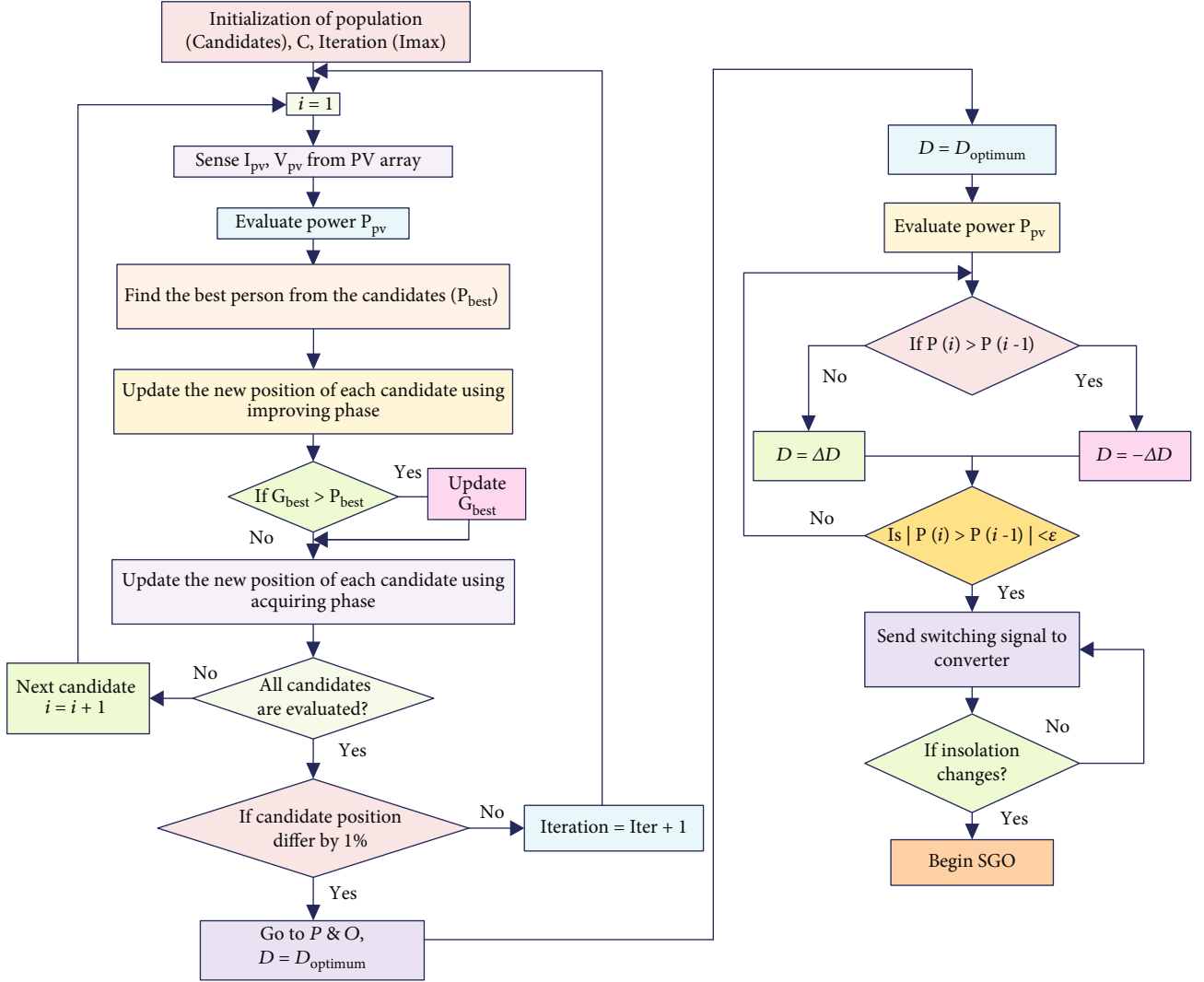


FIGURE 6: Flowchart of the proposed hybrid SGO-PO MPPT algorithm.

TABLE 1: Comprehensive description of the shading pattern.

Various Patterns	Solar Irradiance ( $W/m^2$ )			PV 4	$P_{max}$ (W)
	PV 1	PV 2	PV3		
Pattern 1	1000; 700; 300	1000; 700; 300	1000; 700; 300	1000; 700; 300	798; 557.8; 227.3
Pattern 2	500	800	1000	900	504.2
Pattern 3	800	300	700	500	322.2

the presence of nearby power peaks. Hence, any algorithm used should not only prevail over the local peaks but also should converge within short period with good accuracy. The rational idea of hybridizing MPPT schemes helps to avoid unneeded global searches on transient shading.

### 3. Formulation of the Optimization Problem

The optimized value of the duty cycle is defined by the intelligent MPPT algorithm by formulating the conditions for achieving maximum power. The duty ratio  $d$  of the DC-

DC converter is a variable that is confined for value through the conditions given in (4).

$$\text{Maximize } P_{pv}(d), \quad (3)$$

$$\text{Subject to : } d_{min} \leq d \leq d_{max}, \quad (4)$$

where  $P_{pv}$  is the PV output power,  $d$  is the duty ratio of DC-DC converter,  $d_{max}$  is the maximum limit of duty ratio, and  $d_{min}$  is the minimum limit of duty ratio. The objective function in this context is to maximize the output

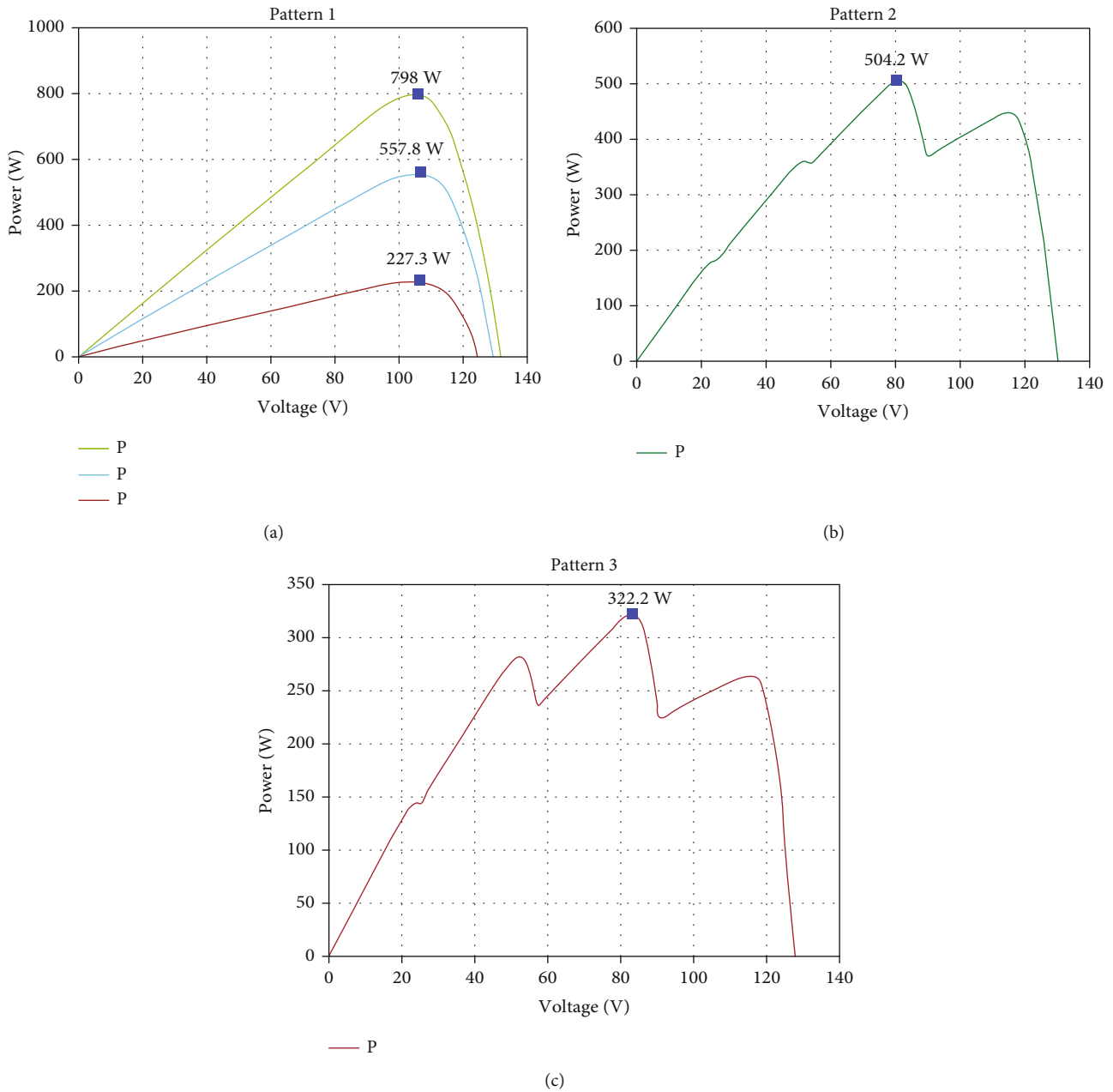


FIGURE 7: P-V Curve. (a) Pattern 1. (b) Pattern 2. (c) Pattern 3.

power of the photovoltaic system. The output power of the PV system is directly related to the duty cycle of the DC-DC converter used in the system. The converter's duty cycle controls the transfer of power from the PV panels to the load or storage system. The goal is to find the optimal duty cycle that allows the PV system to operate at its maximum power point (MPP). To evaluate the fitness of a candidate solution (duty cycle), the duty cycle is applied in the DC-DC converter, and upon the settling of the power for the given duty cycle, the same is fed back to the algorithm as the fitness corresponding to that candidate solution. Upon updating the position of the candidate to the new position, the new position is validated against boundary condition. In case the new position is above or below the upper

bound or lower bound, respectively, the new position is reset to the corresponding upper or lower bound.

**3.1. Social Group Optimization- (SGO-) Based MPPT.** The SGO method performs optimization in two distinct phases. In the first step, the acquaintance of each distinct candidate is enhanced by the influence obtained from the person in the group who is the most qualified. During the second phase, each applicant will have the opportunity to increase their knowledge through reciprocal interaction of their fellow candidates inside the group, as well as with the individual who is regarded as the best overall inside the cluster. The first phase is known as the enhancing phase, while the



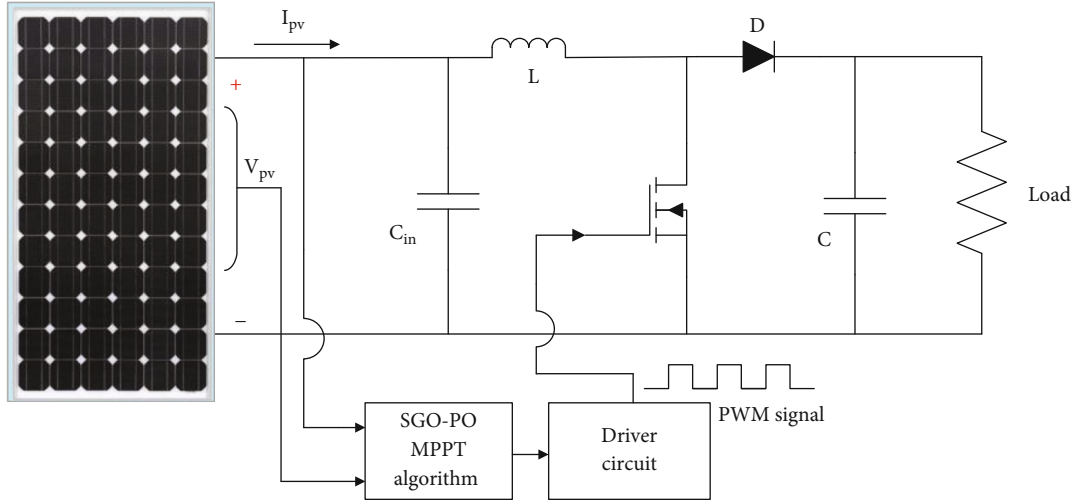


FIGURE 8: Block diagram of test system for the proposed Hybrid-MPPT method.

second phase is known as the acquiring phase. The symbol  $N$  represents the total number of individuals in the group, and each individual person is denoted by the symbol  $X_k$ , where  $k$  is the number of a certain candidate that is present in that group.  $f_k$  ( $k = 1, 2, \dots, N$ ) is the related fitness of the candidate, which is denoted by the  $X_{kD}$  notation, which refers to the candidate's dimension, which is a reference to the individual's characteristics.

**3.1.1. Improving Phase.** In this stage of the process, the best candidate from each social group becomes known as the global best ( $G_{best}$ ) and aims to share their expertise with the other members of the team. Members of the team who take part in this learning process will have their existing expertise enhanced. In addition, candidates will be communicating with one another during this phase to update the information after each repeat and share what they know with one another. Equation (5) might be used to illustrate this process shown in Figures 3(a) and 3(b).

$$D_{new} = C * D_{old} + r(D_{best} - D_{old}), \quad (5)$$

where  $r$  is the random number,  $D_{new}$  is the new fitness, and  $D_{new}$  replaces  $D_{old}$  if  $D_{new}$  presents better fitness, and  $C$  is the self-introspection (0 to 1).

**3.1.2. Acquiring Phase.** During this phase, everyone in the group interacts with someone else in the group in a way that is chosen at random. They also get instruction from someone who is very knowledgeable about the subject. Everyone will learn fresh information not just from one another but also from the individual who possesses the most expertise ( $G_{best}$ ). If there is another individual who possesses more information than  $G_{best}$ , replace the best candidate with themselves. Selecting one individual at random  $D_{rand}$ .

$$D_{new} = D + r_1(D - D_{rand}) + r_2(G_{best} - D), \quad (6)$$

If  $D(P_{pv}) > D_{rand}(P_{pv})$ ,

If  $D_{rand}(P_{pv}) > D(P_{pv})$ ,

$$D_{new} = D - r_1(D - D_{rand}) + r_2(G_{best} - D). \quad (7)$$

Accept  $D_{new}$  if it has a better value for the fitness function.  $r_1$  and  $r_2$  are two different random sequences. The use of these sequences impacts the algorithm's stochastic behaviour, as denoted by equations (6) and (7), which explain how this is accomplished and processed as shown in Figure 4.

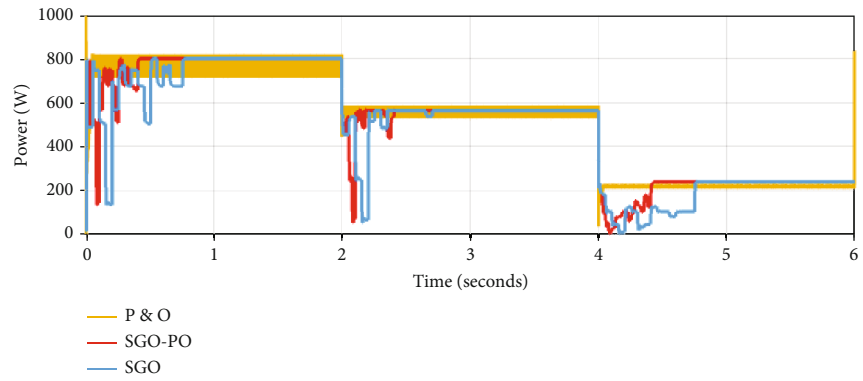
**3.2. Perturb and Observe- (P&O-) Based MPPT.** A P&O MPPT technique tracks MPP by perturbing the operating point and detecting changes in output power from the PV. The P&O-based MPPT algorithm measures PV array voltage and current to determine the power. Then, based on power fluctuation, it perturbs the duty cycle.

$$d_{new} = d_{old} + \Phi, \quad (8)$$

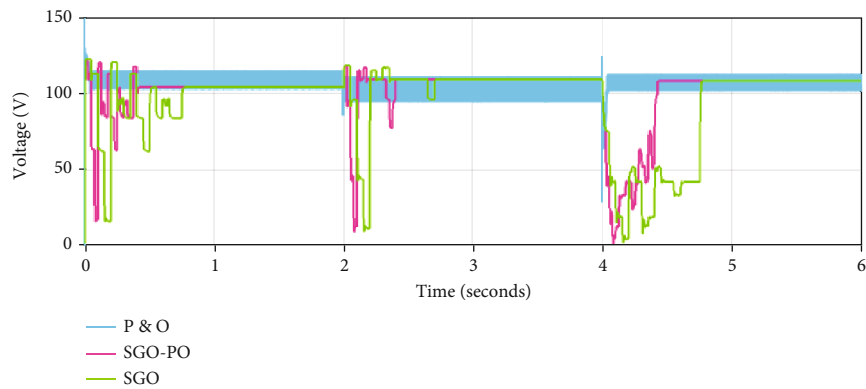
$$d_{new} = d_{old} - \Phi. \quad (9)$$

where  $\Phi$  denotes the perturbed duty cycle. Convergence occurs more quickly, and steady-state oscillation increases if  $\Phi$  is large, while the opposite is true if  $\Phi$  is small.

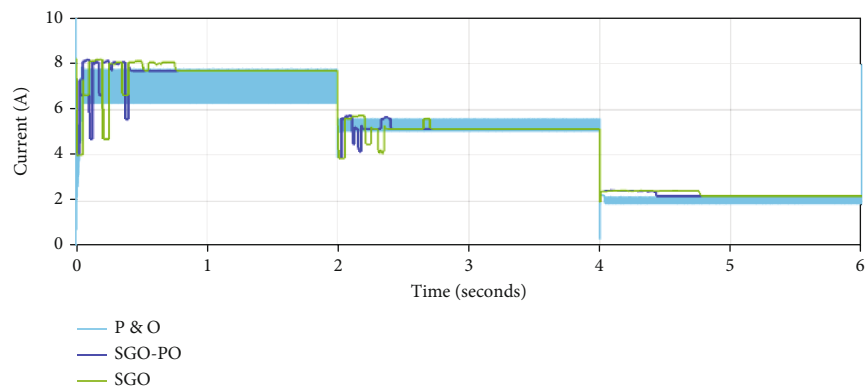
**3.3. Proposed Hybrid-MPPT.** To prevent any ambiguity that may arise during the transition from homogeneous to nonhomogenous or vice versa, a hybrid optimization method using an SGO and a P&O-based MPPT techniques have been developed in this paper. In uniform insolation, the P&O MPPT is activated to follow the MPP, but in nonuniform insolation, the hybrid MPPT follows the global power peak by initiating the SGO first, and then tracking happens through the P&O MPPT method. For a PV array that is highly prone to partially shading, the suggested SGO-PO hybrid-MPPT is appropriate, and it ensures improvement in the power yield as well on the swift tracking of the global power peak. The proposed MPPT method discards the usage of the PI control loop as the duty cycle is generated from the algorithm itself and it is rendered to the DC-DC converter. The computational effort required to tune the controller's gain is diminished, and the controller itself is made simpler as a result. While increasing the number of candidates improves MPP accuracy, it also significantly



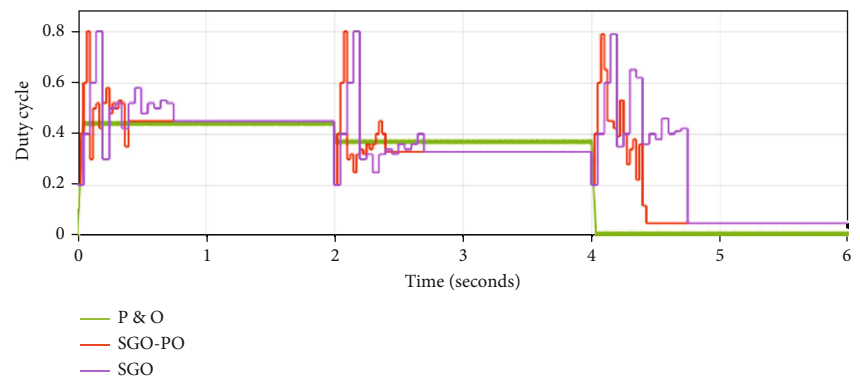
(a)



(b)

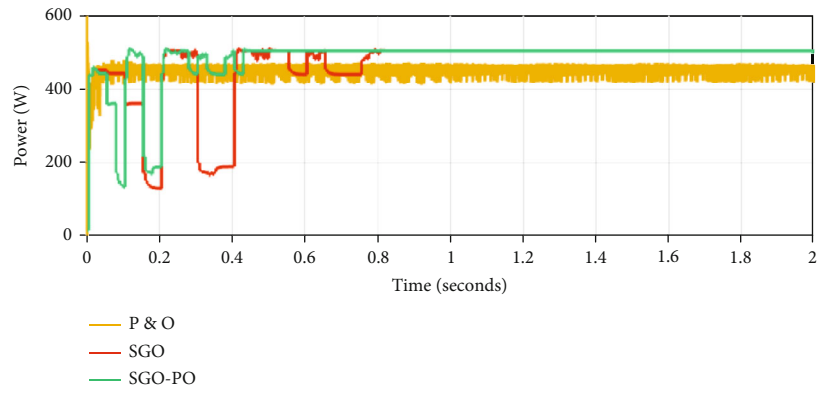


(c)

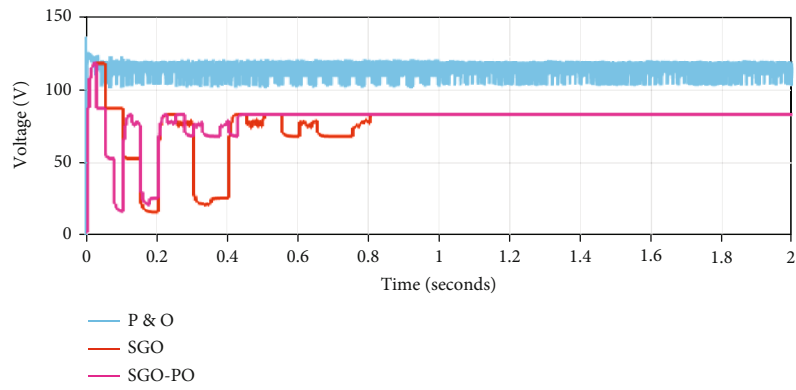


(d)

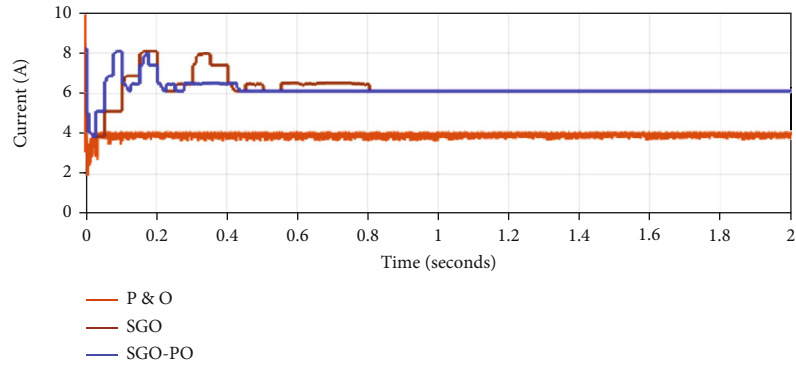
FIGURE 9: Simulation results of rapidly changing insolation pattern 1.



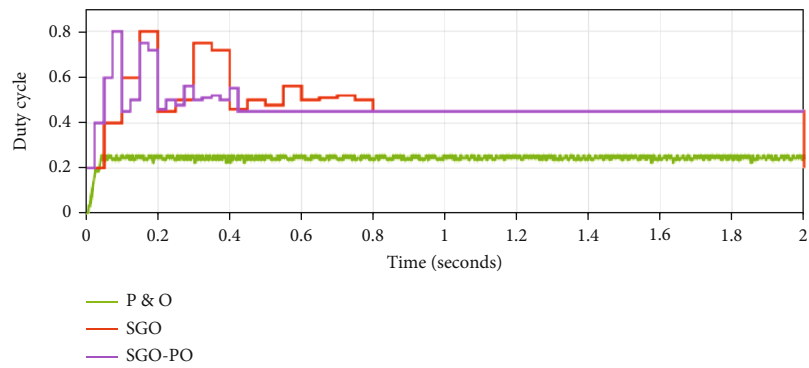
(a)



(b)

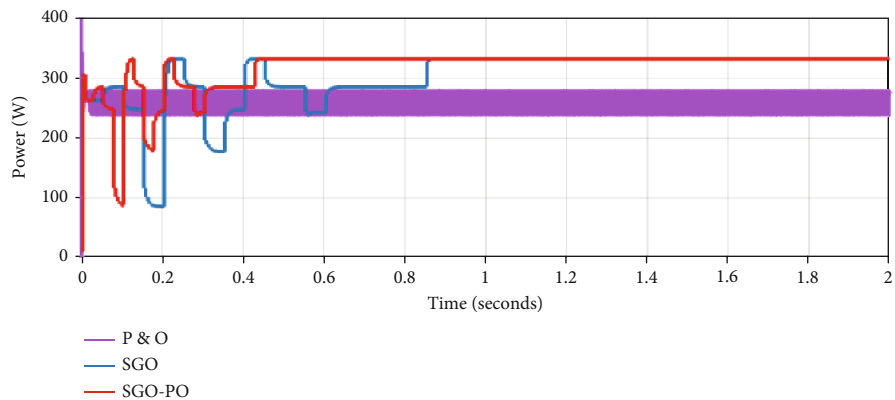


(c)

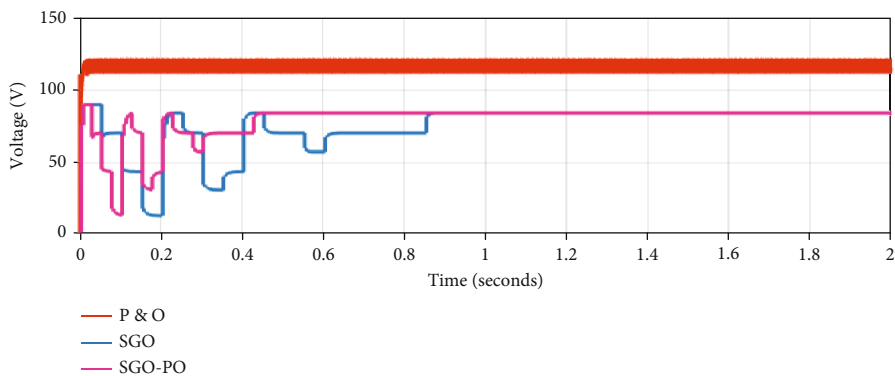


(d)

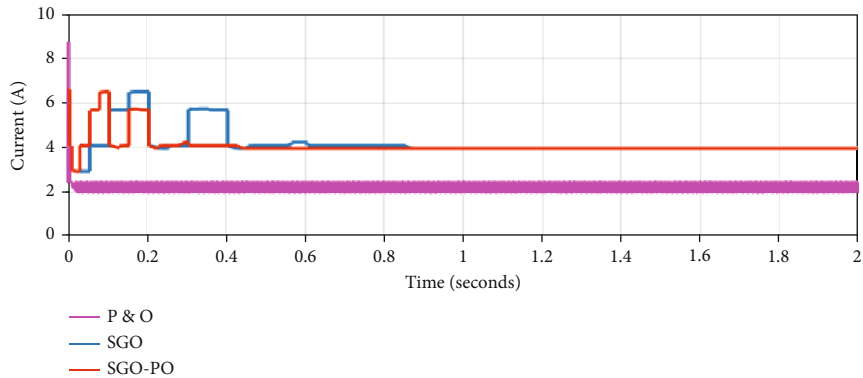
FIGURE 10: Simulation results of partial shading pattern 2.



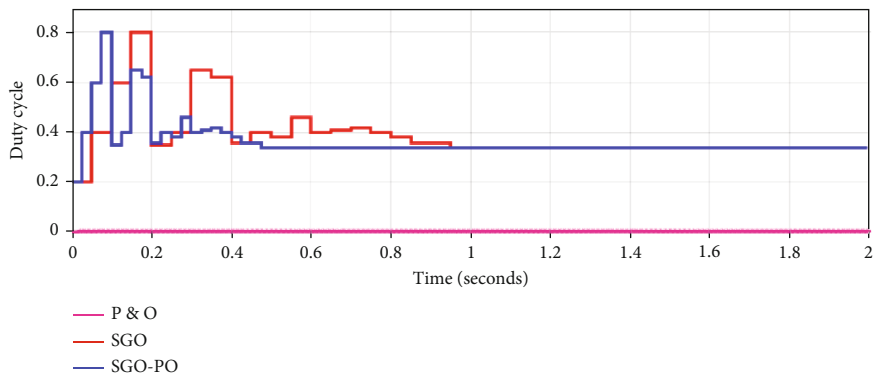
(a)



(b)



(c)



(d)

FIGURE 11: Simulation results of partial shading pattern 3.

TABLE 2: Performance analysis-comparison results.

Algorithm	Cases	Iterations	Convergence time (s)	Power at GM (W)	Power tracked (W)	Efficiency (%)
P&O	Pattern1	—	0.05	798, 557.8, 227.3	790, 550,223	98.20
	Pattern2	—	—	504.2	440.5	87.36
	Pattern3	—	—	322.2	265	82.24
SGO	Pattern1	7	0.75	798, 557.8, 227.3	797.5, 557.3, 226.8	99.91
	Pattern2	10	0.8	504.2	503.5	99.86
	Pattern3	12	0.82	322.2	321.5	99.78
SGO-PO	Pattern1	3	0.40	798, 557.8,227.3	797.7,557.5,227	99.93
	Pattern2	4	0.41	504.2	503.8	99.92
	Pattern3	5	0.43	322.2	321.9	99.90

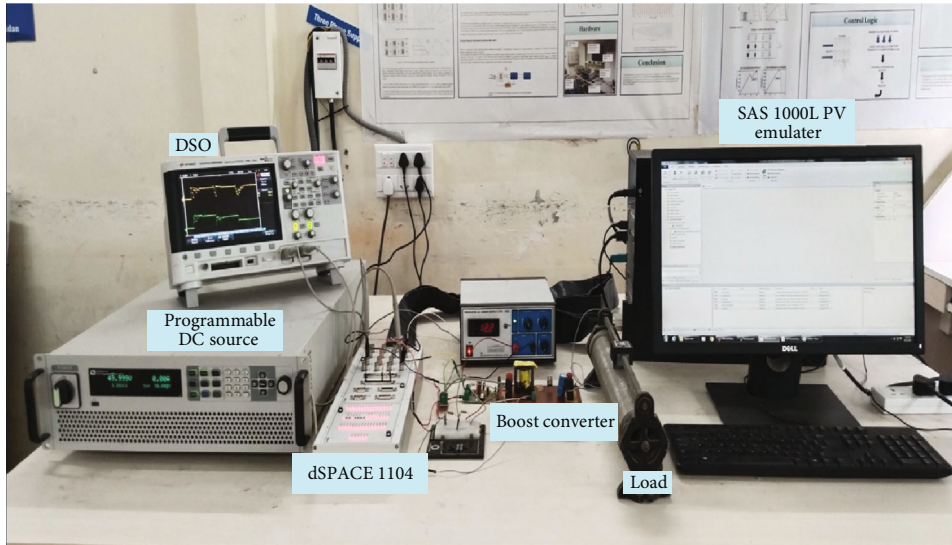


FIGURE 12: Experimental setup for the validation of the proposed hybrid algorithm.

increases the computing load. As a result, to save time, the maximum number of potential candidates might be set at 3. The proposed hybrid-MPPT method is illustrated through several steps as follows:

*Step 1:* initialization. Initialize the population (duty ratio) size = 3. Initialize the parameter  $C = C_{\max} - l(C_{\max} - C_{\min}/L)$ , where  $C_{\max}$  and  $C_{\min}$  are the maximum and minimum value of  $C$ , respectively.  $l$  is the current iteration.  $L$  is the maximum no. of iteration.

*Step 2:* evaluate fitness of each candidate  $V_{pv} * I_{pv} = P_{pv}$ .

*Step 3:* find the best candidate who has more power from the all the candidates using improving phase and acquiring phase.

*Step 4:* repeat the steps 2 and 3 until all candidates converge to MPP with less than 1% duty cycle variation.

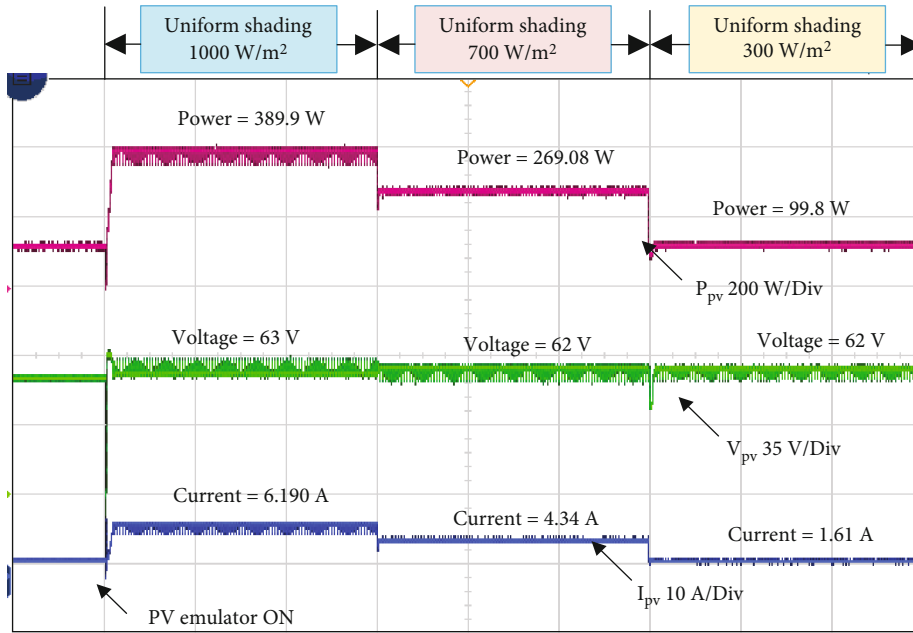
*Step 5:* after locating the MPP, start the P&O loop to track maximum power after finding the MPP global peak (GP). Small step sizes minimize PV output power fluctuations and improve tracking efficiency.

Figure 5 shows the P-V curves for the dynamic changes in solar irradiation. Both Figures 5(a) and 5(b) depict that for a uniform irradiation of  $1000 \text{ W/m}^2$ , the peak power is

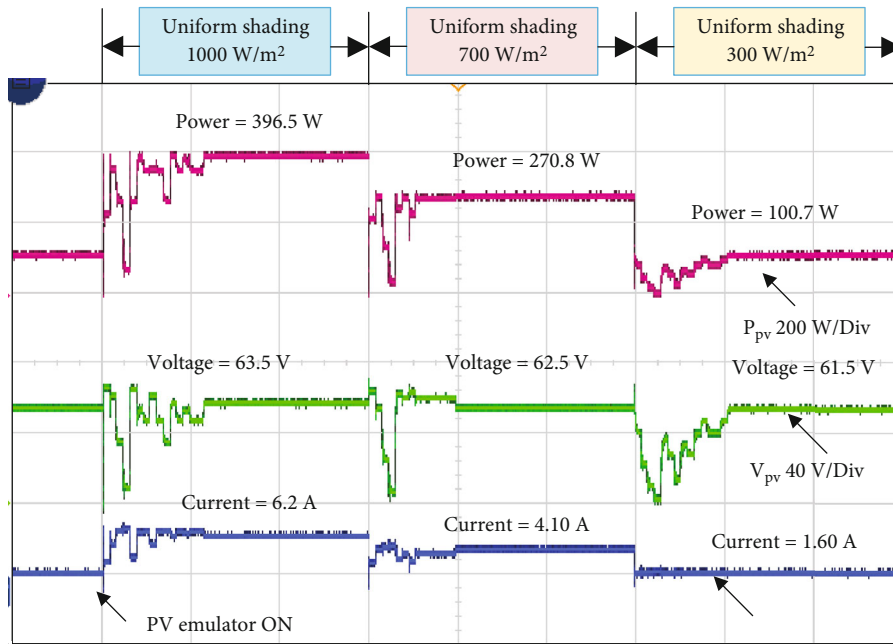
800 W. The 800 W is the global maximum power peak. When a sudden shading affects the PV array, the individual panel in the array exhibits different operating voltage and current, and as cumulative P-V curve, it will have multiple power peaks as shown in the figures. The SGO, through its search process, ensures the optimum duty cycle near the peak power, and P&O sweeps the remaining area and achieves the peak power convincingly. In the flowchart, the left side segment depicts the process of SGO, and the right side shows the P&O MPPT as shown in Figure 6.

#### 4. Simulation and Experimental Validation Results, and Discussions

To check the versatility of the search process, three shading patterns are applied to the PV array as shown in Table 1, with the respective shading pattern power-voltage curve shown in Figure 7. These shading pattern simulations and experimental tests have been carried out. The condition to have a transition from SGO to P&O search is achieving optimum duty cycle, say  $D$  optimum where there will not be an appreciable change in the duty value between the previous



(a)



(b)

FIGURE 13: Continued.

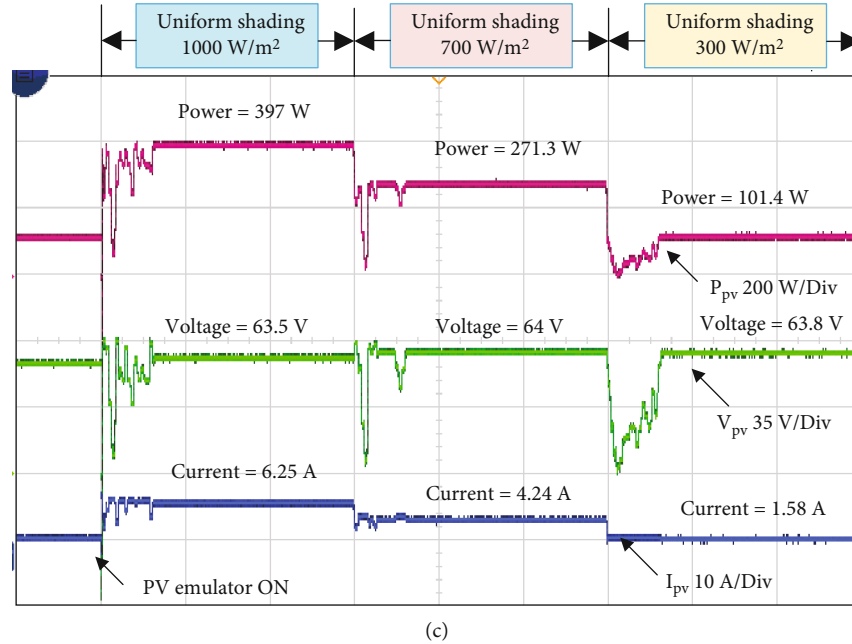


FIGURE 13: Hardware results of rapidly varying irradiation pattern 1. (a) P&O. (b) SGO. (c) SGO-PO.

iteration and the current one. In addition, the power variations should be limited within 10% of its optimum value. Once the P&O takes control, the search process becomes a linear one and the peak power is reached in no time without much oscillations. The competence of the proposed hybrid MPPT for the PV array taken for the study is subjected to both dynamically varying irradiation and partially shaded cases, and the simulation is done in the MATLAB® 2022a and Simulink® platform. Figure 8 shows the test system which includes a PV array, a DC-DC boost converter, an MPPT controller, and a resistive load.

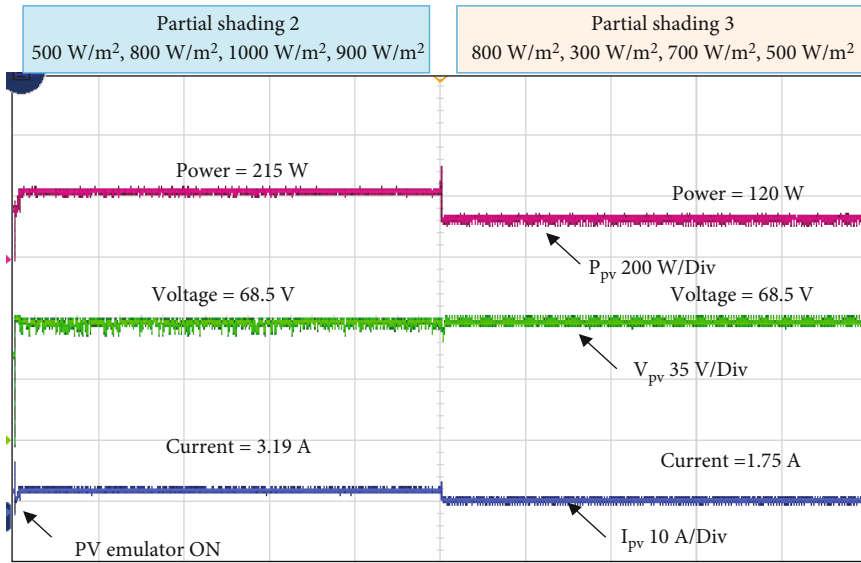
The specifications of the PV panel and details of the DC-DC converters are as follows:  $P_{max} = 200$  W,  $V_{oc} = 32.8$  V,  $I_{sc} = 8.21$  A,  $V_{mp} = 26.3$  V,  $I_{mp} = 7.61$  A,  $C_{in} = 15$   $\mu$ F,  $L = 369.25$   $\mu$ H,  $C_{out} = 14.45$   $\mu$ F and  $R = 13.83$   $\Omega$ .

**4.1. Performance Analysis for Varying Insolation Patterns.** In the context of performance analysis, the efficiency of maximum power point tracking (MPPT) algorithms is typically defined as the ratio of the actual power output of a photovoltaic (PV) system to the maximum possible power that the system could generate under specific conditions. The specific formula used to calculate the efficiency of MPPT algorithms is shown in equation (10). The actual power is calculated with current ( $I_{actual}$ ) and voltage ( $V_{actual}$ ) upon termination condition of reaching the MPP. The maximum power point (MPP) is the point on the current-voltage ( $I$ - $V$ ) curve of the PV system where the product of current maximum ( $I_{max}$ ) and voltage maximum ( $V_{max}$ ). The MPPT scheme is adopted to ensure the operation of the PV panel at MPPT. It is noteworthy that the efficiency of MPPT algorithms can vary depending on factors such as weather conditions, PV panel characteristics, and the algorithm's tracking speed and accuracy. Therefore, performance analysis often

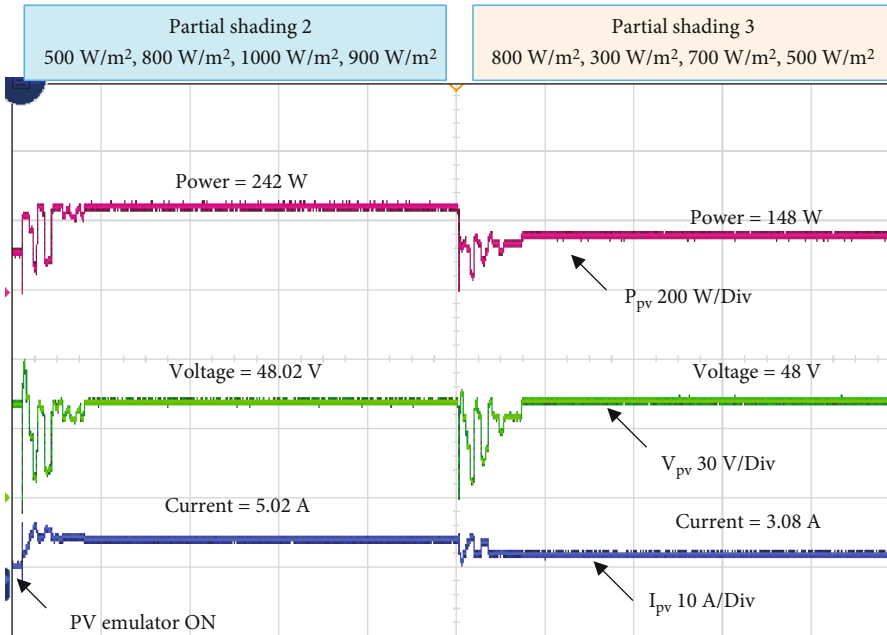
involves testing the algorithm under various conditions to evaluate its effectiveness and efficiency.

**4.1.1. Rapidly Changing Insolation Pattern 1.** In pattern 1, a varying irradiation pattern given in Table 1 has been applied with a dynamic time variation of 2 sec. The global peak powers for this shading pattern are found to be 798 W, 557.8 W, and 227.3 W corresponding to the solar irradiance of 1000, 700, and 300 W/m<sup>2</sup>, respectively. Figure 9(a) shows the maximum power tracking transient response with pattern 1. The SGO-PO MPPT acquires a peak power of 795.7 W, whereas the SGO MPPT tracks 797.5 W and the PO MPPT could only track 790 W. Apparently, the SGO-PO possesses a better tracking efficiency of 99.93%, whereas the SGO MPPT and PO MPPT has a lesser tracking efficiency of 99.91% and 98.20%, respectively. Similarly, the convergence of this SGO-PO MPPT is 0.40 s when compared to its counterparts values are 0.75 s and 0.05 s, respectively. Though the PO MPPT has less convergence time, it has huge power oscillations in the output. The temporal evolution of  $V_p$ ,  $I_p$ , and duty cycle  $d$  is depicted in Figures 9(b)–9(d).

**4.1.2. Partial Shading Pattern 2.** To represent a partially shaded environment, a nonuniform irradiation profile of 500 W/m<sup>2</sup>, 800 W/m<sup>2</sup>, 1000 W/m<sup>2</sup>, and 900 W/m<sup>2</sup> has been introduced. Figures 10(a)–10(d) show the performance of the tracking operations. The P&O MPPT scheme can only track a local minimum of 440.5 W out of the global peak of 504.2 W. The SGO-PO MPPT captures a peak power of 503.8 W, compared to SGO MPPT wherein grasps 503.5 W. With respect to the convergence time, SGO-PO attains 0.41 s to settle, but SGO takes 0.80 s. In terms of efficiency, SGO-PO, SGO, and P&O in the output make this MPPT a lesser performed are 99.92%, 99.91%, and 87.36%, respectively.



(a)



(b)

FIGURE 14: Continued.



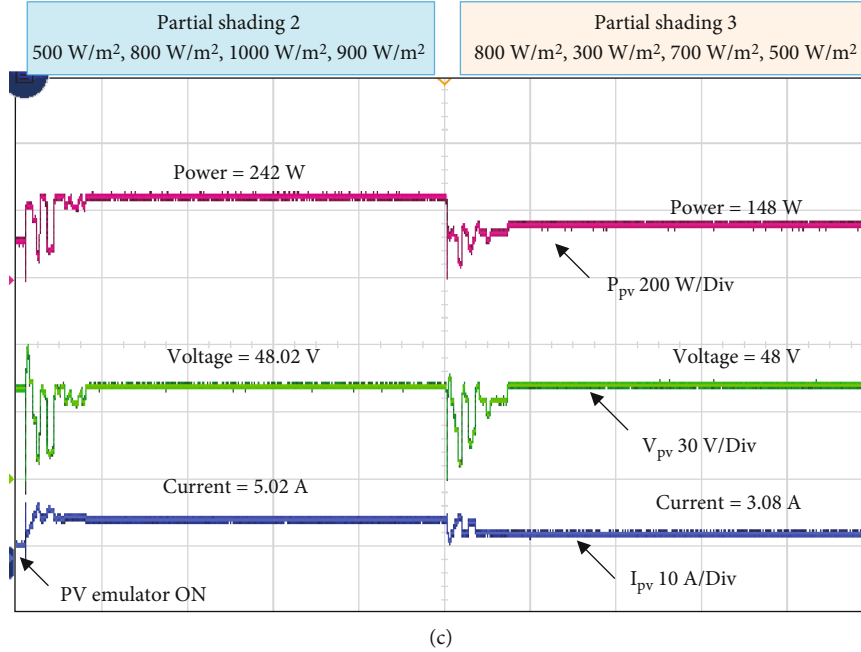


FIGURE 14: Hardware results of partial shading pattern 2 and pattern 3. (a) P&O. (b) SGO. (c) SGO-PO.

**4.1.3. Partial Shading Pattern 3.** In this case, panels 1, 2, 3, and 4 receive the shading pattern of  $800 \text{ W/m}^2$ ,  $300 \text{ W/m}^2$ ,  $700 \text{ W/m}^2$ , and  $500 \text{ W/m}^2$ , respectively. The actual global MPP for this shading pattern is  $322 \text{ W}$ . Figure 11 shows how each algorithm responds when it tries to track the maximum power. The SGO hybrid MPPT successfully grasps the peak power of  $321.9 \text{ W}$ , SGO is  $321.5 \text{ W}$ , and P&O is  $265$  (local maximum), and their efficiencies are found to be  $99.90\%$ ,  $99.78\%$ , and  $82.24\%$ , respectively. The SGO-PO, SGO, and P&O had convergence times of  $0.43$ , and  $0.82$ , and the P&O stuck at local maximum.

$$\% \eta_{\text{static}} = \frac{P_{\text{PV}}}{P_{\text{mp}}} \times 100, \quad (10)$$

where  $P_{\text{PV}}$  is the power measured at steady-state and  $P_{\text{mp}}$  is the actual maximum power.

Table 2 shows the findings of the statistical analysis of the three MPPT algorithms. The efficiency is calculated as shown in (10). The comparison was conducted with consideration of the three patterns described earlier.

**4.2. Experimental Implementation and Results.** Figure 12 shows the hardware arrangement of the SGO MPPT method. The setup necessarily consists of a PV emulator—a DC programmable source, a boost converter (inductance  $-470 \mu\text{H}$ , capacitance  $-150 \mu\text{F}$ ), a dSPACE DS-1104 controller, and a load resistance—( $50 \Omega$ ). A  $400 \text{ W}$  PV array with partial shading is configured through the SAS 1000 L PV emulator. The specifications of the PV panel are as follows:  $P_{\text{max}} = 100 \text{ W}$ ,  $V_{\text{oc}} = 21.5 \text{ V}$ ,  $I_{\text{sc}} = 6.97 \text{ A}$ ,  $V_{\text{mp}} = 16.5 \text{ V}$ , and  $I_{\text{mp}} = 6.3 \text{ A}$ . The emulated values are fed to the programmable DC source (IT6005B). The programmable source renders

the PV array's real-time current and voltage values in accordance with the shading pattern. The change in irradiation pattern results in changes in current and voltage values. The measuring instrument essentially has a WCS1700 current sensor which is employed to find the current value corresponding to the irradiation value, a voltage divider by appropriate resistances that fetch the voltage of the PV array for respective irradiation. The dSPACE controller receives the current input through ADC1 and voltage input through ADC2. The dSPACE feeds these values to the SGO MPPT algorithm in the MATLAB environment. The duty cycle relevant to the global power peak is exerted out through slave I/O 7th pin of dSPACE controller. The driver unit, to amplify the control signal, a TLP 250 driver unit is used, and the output of the driver is given to the boost converter MOSFET IRF460.

**4.2.1. Rapidly Changing Insolation Pattern 1.** Figure 13 presents case 1 where the PV array is exposed to uniform illumination, and there will be only a change in the magnitude of the irradiation with respect to time. During uniform irradiation of  $1000 \text{ W/m}^2$ , the peak power tracked is  $397 \text{ W}$ , and for  $700 \text{ W/m}^2$ , it is  $271.3 \text{ W}$ . Also, when the irradiation is low as  $300 \text{ W/m}^2$ , the power attained is  $101.4 \text{ W}$ , the corresponding operating voltage is  $61.5 \text{ V}$ , and the operating current is  $1.65 \text{ A}$ . The tracking efficiency for this shading pattern is  $99.7\%$ . It is interesting to note that in the power curve, initially SGO converges at  $0.60 \text{ s}$ , and from there on, the PO MPPT comes into operating and tracks the peak power of  $397 \text{ W}$ . The convergence time is reduced due to this operation, and the reliability of the search process is increased.

**4.2.2. Partial Shading Pattern 2 and Pattern 3.** The SGO-PO hybrid MPPT shows its versatility when the PV array is shaded dynamically. Pattern 2 and pattern 3 have been

TABLE 3: Performance analysis experimental results.

Algorithm	Cases	Convergence time (s)	Power at GM (W)	Power tracked (W)	Efficiency (%)
P&O	Pattern1	0.5	398, 273.5, 102.5	389.9, 269.08, 99.8	97.9
	Pattern2	—	243.5	215	88.29
	Pattern3	—	150	120	80
SGO	Pattern1	1.3	398, 273.5, 102.5	396.5, 270.8, 100.7	99.4
	Pattern2	1.8	243.5	241.5	99.1
	Pattern3	1.9	150	147.5	98.3
SGO-PO	Pattern1	0.6	398, 273.5, 102.5	397, 273.5, 101.4	99.7
	Pattern2	0.75	243.5	242	99.3
	Pattern3	0.8	150	148	98.6

applied to PV array to simulate two different shading conditions. Figure 14 shows the experimental results with partial shading in 2 and 3. In pattern 2, each of the four panels is exposed to different irradiation, say panel 1 receives  $500 \text{ W/m}^2$ , panel 2 receives  $800 \text{ W/m}^2$ , panel 3 receives  $1000 \text{ W/m}^2$ , and panel 4 receives  $900 \text{ W/m}^2$ . The global maximum inferred for the cumulative P-V curve is  $243.5 \text{ W}$ . The hybrid MPPT scheme successfully grasps the power of  $242 \text{ W}$  with an operating voltage of  $48.02 \text{ V}$  and an operating current of  $5.02 \text{ A}$  as shown in Figures 14(b) and 14(c). Similarly, for pattern 3, the shading pattern, panel 1 receives  $800 \text{ W/m}^2$ , panel 2 receives  $300 \text{ W/m}^2$ , panel 3 receives  $700 \text{ W/m}^2$ , and panel 4 receives  $500 \text{ W/m}^2$ , and the cumulative global peak for this shading pattern is found to be  $150 \text{ W}$ . The SGO hybrid MPPT successfully grasps the peak power of  $148$  with an efficiency of  $99\%$ . The corresponding voltage and current values are  $48 \text{ V}$  and  $3.08 \text{ A}$  as shown in Figures 14(b) and 14(c).

Table 3 shows the comparative results of convergence towards the global power peak. The performance of the algorithms SGO, P&O, and hybrid SGO-PO has been compared for various shading patterns, and it is inferred that the SGO-PO possesses an optimum efficiency with the higher convergence speed. The difference between SGO and SGO-PO is very small, i.e.,  $0.3\text{-}0.2\%$ . However, such small margins can prove to be very effective at large scales [36]. Furthermore, SGO-PO has a better convergence time showing that the proposed algorithm is not only more efficient but also faster.

## 5. Conclusion

The usage of MPPT is indispensable as far as renewable energy PV is considered. These MPPT schemes become unreliable when the PV array is shaded even partially as they are prone to get stuck with local power peak and not tracking the global ones. The global search algorithms, though competent in grasping the global best power, are not capable of dealing with these partial shading situations. To address this knowledge gap, a novel hybrid SGO-PO MPPT approach has been presented in this paper. The simulation and experimental validation results prove that the tracking mechanism is not only reliable in grasping the global peak power but also swift in convergence. The performance of the suggested schemes is compared with the SGO and

P&O MPPT schemes. The results of various test cases with dynamic irradiation patterns validate that the proposed SGO-PO MPPT scheme. The SGO-PO scheme when tested for the more complex shaded condition (pattern 3) converges within 5 iterations and consumes only  $0.43 \text{ sec}$  to grasp  $321.9 \text{ W}$  with a tracking efficiency of  $99.9\%$  compared to SGO which takes 12 iterations and  $0.8 \text{ secs}$  to converge with a relatively lower tracking efficiency.

## Data Availability

No underlying data was collected or produced in this study.

## Conflicts of Interest

The authors declare no conflict of interest.

## Authors' Contributions

All authors contributed equally to this work.

## References

- [1] T. S. Ustun, Y. Nakamura, J. Hashimoto, and K. Otani, "Performance analysis of PV panels based on different technologies after two years of outdoor exposure in Fukushima, Japan," *Renewable Energy*, vol. 136, pp. 159–178, 2019.
- [2] C. Vimalarani and N. Kamaraj, "Improved method of maximum power point tracking of photovoltaic (PV) array using hybrid intelligent controller," *Optik*, vol. 168, pp. 403–415, 2018.
- [3] A. O. Baba, G. Liu, and X. Chen, "Classification and evaluation review of maximum power point tracking methods," *Sustainable Futures*, vol. 2, article 100020, 2020.
- [4] V. Srinivasan, C. S. Boopathi, and R. Sridhar, "A new meerkat optimization algorithm based maximum power point tracking for partially shaded photovoltaic system," *Ain Shams Engineering Journal*, vol. 12, no. 4, pp. 3791–3802, 2021.
- [5] D. Sera, L. Mathe, T. Kerekes, S. V. Spataru, and R. Teodorescu, "On the perturb-and-observe and incremental conductance MPPT methods for PV systems," *IEEE Journal of Photovoltaics*, vol. 3, no. 3, pp. 1070–1078, 2013.
- [6] S. Manna and A. K. Akella, "Comparative analysis of various P & O MPPT algorithm for PV system under varying radiation

- condition,” in *2021 1st International Conference on Power Electronics and Energy (ICPEE)*, Bhubaneswar, India, 2021.
- [7] R. Singh and P. Basak, “Modelling and simulation of a PV generator and MPPT using P&O method and fuzzy logic controller,” *International Journal of Advanced Research in Electrical, Electronics and Instrumentation Engineering*, vol. 4, no. 7, pp. 5827–5835, 2015.
  - [8] J. Ahmad, “A fractional open circuit voltage based maximum power point tracker for photovoltaic arrays,” in *2010 2nd International Conference on Software Technology and Engineering*, San Juan, PR, USA, 2010.
  - [9] M. Asim, M. Tariq, M. A. Mallick, I. Ashraf, S. Kumari, and A. K. Bhoi, “Critical Evaluation of Offline MPPT Techniques of Solar PV for Stand-Alone Applications,” in *Advances in Smart Grid and Renewable Energy*, S. SenGupta, A. Zobaa, K. Sherpa, and A. Bhoi, Eds., vol. 435 of Lecture Notes in Electrical Engineering, Springer, Singapore, 2018.
  - [10] A. I. M. Ali and H. R. A. Mohamed, “Improved P&O MPPT algorithm with efficient open-circuit voltage estimation for two-stage grid-integrated PV system under realistic solar radiation,” *International Journal of Electrical Power & Energy Systems*, vol. 137, article 107805, 2022.
  - [11] L. Shang, H. Guo, and W. Zhu, “An improved MPPT control strategy based on incremental conductance algorithm,” *Protection and Control of Modern Power Systems*, vol. 5, no. 1, 2020.
  - [12] A. H. Chander, K. D. Rao, B. P. Teja et al., “A transformerless photovoltaic inverter with dedicated MPPT for grid application,” *IEEE Access*, vol. 11, pp. 61358–61367, 2023.
  - [13] A. N. Ali, M. H. Saied, M. Z. Mostafa, and T. M. Abdel-Moneim, “A survey of maximum PPT techniques of PV systems,” in *2012 IEEE Energytech*, Cleveland, OH, USA, 2012.
  - [14] C. Charin, D. Ishak, M. A. Mohd Zainuri, B. Ismail, T. Alsuwian, and A. R. Alhawari, “Modified levy-based particle swarm optimization (MLPSO) with boost converter for local and global point tracking,” *Energies*, vol. 15, no. 19, p. 7370, 2022.
  - [15] J. P. Ram, T. S. Babu, and N. Rajasekar, “A comprehensive review on solar PV maximum power point tracking techniques,” *Renewable and Sustainable Energy Reviews*, vol. 67, pp. 826–847, 2017.
  - [16] J. B. Basu, S. Dawn, P. K. Saha, M. R. Chakraborty, and T. S. Ustun, “A comparative study on system profit maximization of a renewable combined deregulated power system,” *Electronics*, vol. 11, no. 18, p. 2857, 2022.
  - [17] N. Aouchiche, M. S. Aitcheikh, M. Becherif, and M. A. Ebrahim, “AI-based global MPPT for partial shaded grid connected PV plant via MFO approach,” *Solar Energy*, vol. 171, pp. 593–603, 2018.
  - [18] J. P. Ram and N. Rajasekar, “A novel flower pollination based global maximum power point method for solar maximum power point tracking,” *IEEE Transactions on Power Electronics*, vol. 32, no. 11, pp. 8486–8499, 2017.
  - [19] G. S. Patil, A. Mulla, S. Dawn, and T. S. Ustun, “Profit maximization with imbalance cost improvement by solar PV-battery hybrid system in deregulated power market,” *Energies*, vol. 15, no. 14, p. 5290, 2022.
  - [20] P. Gupta, S. Tripathi, S. Singh, and V. S. Gupta, “MPPT-EPO optimized solar energy harvesting for maximizing the WSN lifetime,” *Peer-to-Peer Networking and Applications*, vol. 16, no. 1, pp. 347–357, 2023.
  - [21] A. Soufyane Benyoucef, A. Chouder, K. Kara, and S. Silvestre, “Artificial bee colony based algorithm for maximum power point tracking (MPPT) for PV systems operating under partial shaded conditions,” *Applied Soft Computing*, vol. 32, pp. 38–48, 2015.
  - [22] K. Guo, L. Cui, M. Mao, L. Zhou, and Q. Zhang, “An improved gray wolf optimizer MPPT algorithm for PV system with BFBIC converter under partial shading,” *IEEE Access*, vol. 8, pp. 103476–103490, 2020.
  - [23] A. Das, S. Dawn, S. Gope, and T. S. Ustun, “A strategy for system risk mitigation using FACTS devices in a wind incorporated competitive power system,” *Sustainability*, vol. 14, no. 13, p. 8069, 2022.
  - [24] W. Saad, E. Hegazy, and M. Shokair, “Maximum power point tracking based on modified firefly scheme for PV system,” *SN Applied Sciences*, vol. 4, no. 4, p. 94, 2022.
  - [25] S. Veerapen, H. Wen, X. Li et al., “A novel global maximum power point tracking algorithm for photovoltaic system with variable perturbation frequency and zero oscillation,” *Solar Energy*, vol. 181, pp. 345–356, 2019.
  - [26] M. Alshareef, Z. Lin, M. Ma, and W. Cao, “Accelerated particle swarm optimization for photovoltaic maximum power point tracking under partial shading conditions,” *Energies*, vol. 12, no. 4, p. 623, 2019.
  - [27] M. A. Mohamed, A. A. Z. Diab, and H. Rezk, “Partial shading mitigation of PV systems via different meta-heuristic techniques,” *Renewable Energy*, vol. 130, pp. 1159–1175, 2019.
  - [28] D. Pilakkat and S. Kanthalakshmi, “An improved P&O algorithm integrated with artificial bee colony for photovoltaic systems under partial shading conditions,” *Solar Energy*, vol. 178, pp. 37–47, 2019.
  - [29] M. V. da Rocha, L. P. Sampaio, and S. A. da Silva, “Comparative analysis of MPPT algorithms based on bat algorithm for PV systems under partial shading condition,” *Sustainable Energy Technologies and Assessments*, vol. 40, article 100761, 2020.
  - [30] M. W. Guo, J. S. Wang, L. F. Zhu, S. S. Guo, and W. Xie, “An improved grey wolf optimizer based on tracking and seeking modes to solve function optimization problems,” *IEEE Access*, vol. 8, pp. 69861–69893, 2020.
  - [31] S. Lyden, H. Galligan, and M. E. Haque, “A hybrid simulated annealing and perturb and observe maximum power point tracking method,” *IEEE Systems Journal*, vol. 15, no. 3, pp. 4325–4333, 2021.
  - [32] S. Vadivel, B. C. Sengodan, S. Ramasamy, M. Ahsan, J. Haider, and E. M. Rodrigues, “Social grouping algorithm aided maximum power point tracking scheme for partial shaded photovoltaic array,” *Energies*, vol. 15, no. 6, p. 2105, 2022.
  - [33] V. J. Chin, Z. Salam, and K. Ishaque, “Cell modelling and model parameters estimation techniques for photovoltaic simulator application: a review,” *Applied Energy*, vol. 154, pp. 500–519, 2015.
  - [34] T. S. Ustun, J. Hashimoto, and K. Otani, “Using RSCAD’s simplified inverter components to model smart inverters in power systems,” in *2018 IEEE Workshop on Complexity in Engineering (COMPENG)*, pp. 1–6, Florence, Italy, October 2018.
  - [35] K. S. Tey, S. Mekhilef, M. Seyedmahmoudian, B. Horan, A. T. Oo, and A. Stojcevski, “Improved differential evolution-based MPPT algorithm using SEPIC for PV systems under partial shading conditions and load variation,” *IEEE Transactions on Industrial Informatics*, vol. 14, no. 10, pp. 4322–4333, 2018.
  - [36] A. Q. Al-Shetwi, W. K. Issa, R. F. Aqeil et al., “Active power control to mitigate frequency deviations in large-scale grid-connected PV system using grid-forming single-stage inverters,” *Energies*, vol. 15, no. 6, p. 2035, 2022.